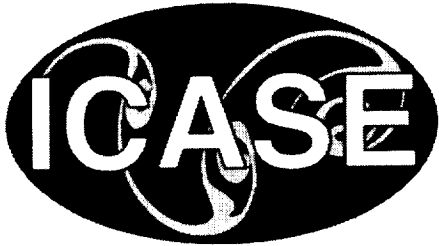


NASA/CR-2002-211655
ICASE Report No. 2002-15



Covolume-based Intergrid Transfer Operator in P_1 Nonconforming Multigrid Method

Kab Seok Kang
ICASE, Hampton, Virginia

ICASE
NASA Langley Research Center
Hampton, Virginia

Operated by Universities Space Research Association



Prepared for Langley Research Center
under Contract NAS1-97046

May 2002

Available from the following:

NASA Center for AeroSpace Information (CASI)
7121 Standard Drive
Hanover, MD 21076-1320
(301) 621-0390

National Technical Information Service (NTIS)
5285 Port Royal Road
Springfield, VA 22161-2171
(703) 487-4650

COVOLUME-BASED INTERGRID TRANSFER OPERATOR IN P_1 NONCONFORMING MULTIGRID METHOD

KAB SEOK KANG*

Abstract. In this paper, we introduce an intergrid transfer operator which is based on the covolume of nodes in a P_1 nonconforming multigrid method and study the convergence behavior of the multigrid method with this intergrid transfer operator. This intergrid transfer operator needs fewer computations and neighborhood node values than previous operators, which is a good property for parallelization. The P_1 nonconforming multigrid method with this intergrid transfer operator is suitable for solving problems with Robin boundary conditions and nonlinear problems with bound constraints on solutions.

Key words. multigrid method, covolume method, nonconforming finite elements, elliptic equations

Subject classification. Applied and Numerical Mathematics

1. Introduction. Multigrid methods are well known as efficient solution techniques for many problems including elliptic and hyperbolic partial differential equations, nonlinear problem, and even systems of algebraic equations that are not derived from the spatial discretization of a partial differential equation ([5, 10, 14, 17]). Because nonconforming finite element or covolume methods have proven flexible and effective on incompressible fluid flow problems and biharmonic and plate problems ([9, 8, 11]) many researchers have been interested in studying multigrid methods for nonconforming finite elements or covolume methods ([6, 7, 2, 4, 1, 12]).

In nonconforming multigrid methods, the intergrid transfer operators have important roles in convergence. In this paper, we consider a covolume-based intergrid transfer operator. This intergrid transfer operator needs less computation and neighborhood node information than previously proposed intergrid transfer operators. The P_1 nonconforming multigrid method with previous intergrid transfer operators is less suitable for solving nonlinear problems that have bounds on solutions and has poor error reduction for problems with Robin boundary conditions. However the P_1 nonconforming multigrid method with this intergrid transfer operator is very suitable for such problems.

Many authors have shown that nonconforming W -cycle multigrid methods converge and nonconforming variable V -cycle multigrid preconditioners have a uniform condition number as preconditioners. In this paper, we investigate the convergence behavior of W -cycle multigrid methods and the condition number as preconditioners of V -cycle multigrid methods with covolume-based intergrid transfer operators, by means of numerical experiments.

This paper is organized as follows. In section 2, we summarize some results of P_1 nonconforming finite element and covolume methods. In section 3, we introduce the covolume-based intergrid transfer operator and recount the abstract theory developed by Bramble et al. for nonnested multigrid methods. In section 4, we report the results of numerical experiments justifying the convergence theory presented in section 3 and applied to a Radiation Transport problem which is a system of coupled nonlinear partial differential equations with discontinuous diffusion coefficients.

*ICASE, Mail Stop 132C, NASA Langley Research Center, Hampton, VA 23681-2199 email: kks002@icase.edu. This research was partially supported by the National Aeronautics and Space Administration under NASA Contract No. NAS1-97046 while the author was in residence at ICASE, NASA Langley Research Center, Hampton, VA 23681-2199. This work was also partially supported by postdoctoral fellowships program from Korea Science & Engineering Foundation (KOSEF).

2. Model problem and its discretizations. We consider the second-order elliptic problem with Robin boundary conditions

$$\begin{aligned} -\nabla \cdot \mathbb{A} \nabla u &= f, & \text{in } \Omega, \\ \beta u + \mathbb{A} \frac{\partial u}{\partial n} &= g, & \text{on } \partial\Omega, \end{aligned} \quad (2.2.1)$$

where $\Omega \in \mathbb{R}^2$ is a bounded polygonal domain with boundary $\partial\Omega$, $f \in L^2(\Omega)$, $g \in L^2(\partial\Omega)$, and the symmetric coefficient matrix $\mathbb{A} \in (L^\infty(\Omega))^{2 \times 2}$ satisfies

$$\alpha_0 \chi^t \chi \leq \chi^t \mathbb{A}(x, y) \chi \leq \alpha_1 \chi^t \chi, \quad (x, y) \in \Omega, \quad \chi \in \mathbb{R}^2, \quad (2.2.2)$$

with fixed constants $\alpha_0, \alpha_1 > 0$. It is well known that if β is not equal to zero on some set of boundary which is not of measure zero, then equation (2.2.1) has a unique solution.

Let $H^s(\Omega)$ and $L^2(\Omega)$ be the usual Sobolev spaces with norm and seminorm

$$\|v\|_s = \left(\int_{\Omega} \sum_{|\alpha| \leq s} |D^\alpha v|^2 dx \right)^{1/2}, \quad |v|_s = \left(\int_{\Omega} \sum_{|\alpha|=s} |D^\alpha v|^2 dx \right)^{1/2},$$

where s is a nonnegative integer. Let (\cdot, \cdot) denote the $L^2(\Omega)$ inner product. As usual, the $L^2(\Omega)$ norm is indicated by $\|\cdot\|_0$.

The variational form of (2.2.1) can be written as follows: Find $u \in H^1(\Omega)$ such that

$$a(u, v) = (f, v) + (g, v)_{\partial\Omega}, \quad \forall v \in H^1(\Omega), \quad (2.2.3)$$

where $a(v, w) = (\mathbb{A} \nabla v, \nabla w) + (\beta v, w)_{\partial\Omega}$, for all $v, w \in H^1(\Omega)$.

Let h_0 and $\mathcal{T}_{h_0} \equiv \mathcal{T}_0$ be given, where \mathcal{T}_0 is a partition of Ω into triangles and h_0 is the maximum diameter of the elements of \mathcal{T}_0 . For each integer $1 \leq k \leq J$, let $h_k = 2^{-k} h_0$ and the sequence of triangulations $\mathcal{T}_{h_k} \equiv \mathcal{T}_k$ be constructed by the nested-mesh subdivision method, i.e., let \mathcal{T}_k be constructed by connecting the midpoints of the edges of the triangles in \mathcal{T}_{k-1} , and let $\mathcal{T}_h \equiv \mathcal{T}_J$ be the finest grid.

Define the P_1 -nonconforming finite element spaces

$$\begin{aligned} V_k &= \{v \in L^2(\Omega) : v|_K \text{ is linear for all } K \in \mathcal{T}_k, \\ &\quad v \text{ is continuous at the midpoints of interior edges}\}. \end{aligned}$$

In P_1 -nonconforming finite elements, the node points are the midpoints of the edges. Obviously, this results in

$$V_0 \not\subset V_1 \not\subset \cdots \not\subset V_J = V_h.$$

Define the bilinear forms over the spaces V_k , for each k , as follows:

$$a_k(v, w) = \sum_{K \in \mathcal{T}_k} (\mathbb{A} \nabla v, \nabla w)_K + (v, w)_{\partial\Omega}, \quad \forall v, w \in V_k,$$

where $(\cdot, \cdot)_K$ is the $(L^2(K))^2$ inner product. Moreover, define the discrete energy norms as follows:

$$\|v\|_{1,k} = a_k(v, v)^{1/2}, \quad \forall v \in V_k.$$

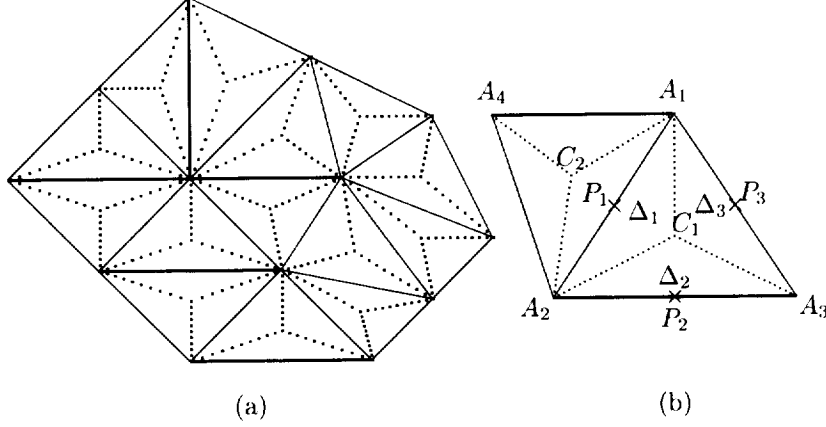


FIG. 1. *Primal and Dual element*

Then the nonconforming finite element discretization equation of (2.2.3) can be written as: Find $u_h \in V_h$ such that

$$a_h(u_h, v_h) = (f, v_h) + (g, v_h)_{\partial\Omega}, \quad v_h \in V_h. \quad (2.2.4)$$

From a previous study of P_1 nonconforming finite element methods [9], we have

$$\|u - u_h\|_0 + h\|u - u_h\|_{1,k} \leq Ch_k^2 |u|_2 \quad (2.2.5)$$

if $u \in H^2(\Omega)$.

To define a covolume of nodes, we construct the dual partitions \mathcal{T}_k^* . Divide each triangle of the primal partition into three sub-triangles by connecting two vertices and the barycenter of a primal element as in Figure 1(a). As in Figure 1(b), the dual element based at the node P_1 (covolume of P_1) is made up of the two triangles $\Delta A_1 C_1 A_2$ and $\Delta A_1 C_2 A_2$. We do the obvious modification at a boundary node. Carrying out the construction for every node in the primal partition, we obtain a dual partition for the domain. We denote the covolume of node P as K_P^* and the dual partition as $\mathcal{T}_k^* = \cup K_P^*$. Define the associated test function spaces Y_k as the space of piecewise constant functions:

$$Y_k = \{z \in L^2(\Omega) : z|_{K_P^*} \text{ is a constant vector}\}.$$

Obviously, we have

$$Y_0 \not\subset Y_1 \not\subset \cdots \not\subset Y_J = Y_h.$$

Define an operator from the spaces $V_k \times Y_k$, for each k , as follows,

$$\begin{aligned} a^*(u_h, v_h) &= - \sum_{i=1}^{N_k} \int_{\partial K_{P_i}^* \setminus \partial K_{P_i}^* \cap \partial\Omega} \mathbb{A} \frac{\partial u_h}{\partial n} v_h d\sigma + \int_{\partial\Omega} \beta u_h v_h d\sigma \\ &= - \sum_{i=1}^{N_k} v_h(P_i) \int_{\partial K_{P_i}^* \setminus \partial K_{P_i}^* \cap \partial\Omega} \mathbb{A} \frac{\partial u_h}{\partial n} d\sigma + \int_{\partial\Omega} \beta u_h v_h d\sigma, \end{aligned} \quad (2.2.6)$$

where $\frac{\partial u_h}{\partial n}$ is the outer normal derivative of u_h .

The covolume discretization equation of (2.2.1) can be written as: Find $u_h^* \in V_h$ such that

$$a_h^*(u_h^*, v_h) = (f, v_h) + (g, v_h)_{\partial\Omega}, \quad \forall v_h \in Y_h. \quad (2.2.7)$$

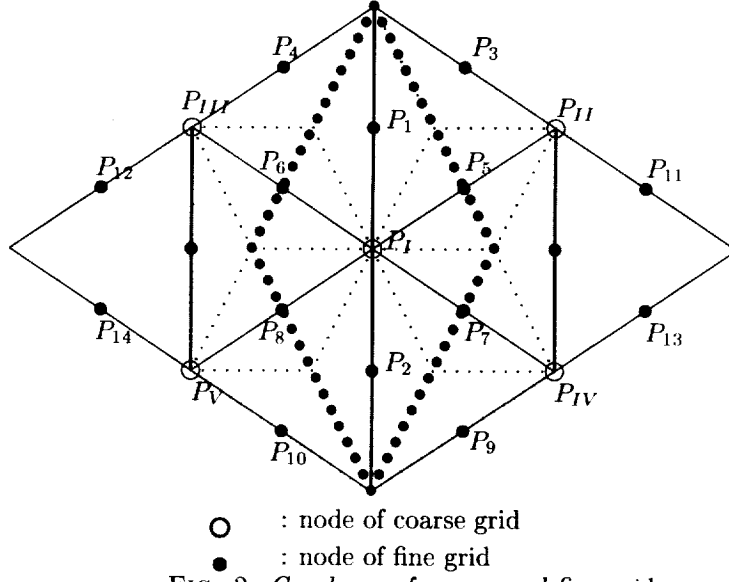


FIG. 2. Covolume of coarse and fine grid

We introduce one-to-one transfer operator γ_k from $V_k \rightarrow Y_k$ by

$$\gamma_k v_h(x) = \sum_{j=1}^{N_k} v_h(P_j) \chi_j^*(x), \quad \forall x \in \Omega, \quad (2.2.8)$$

where χ_j^* is a characteristic function associated with the dual element $K_{P_j}^*$, $j = 1, \dots, N_k$.

If we assume that \mathbb{A} is piecewise constant, then we have the following relation

$$a_k(u_h, v_h) = a_k^*(u_h, \gamma_k v_h), \quad \forall u_h, v_h \in V_k \quad (2.2.9)$$

from [8].

We have the following convergence estimate from [8] and [11]:

$$\begin{aligned} \|u - u_h^*\|_{1,k} &\leq Ch(\|u\|_2 + 1), \quad \text{if } u \in H^2(\Omega), \\ \|u - u_h^*\|_0 &\leq Ch^2(\|u\|_3 + 1), \quad \text{if } u \in H^3(\Omega). \end{aligned} \quad (2.2.10)$$

In the case where \mathbb{A} is piecewise constant, the finite element method and the covolume method differ only in the source term (right-hand side of equation). Therefore, in the next section, we consider only the discretization of the linear problem induced by the finite element method.

3. Multigrid method and covolume-based intergrid transfer operator. In this section, we introduce a covolume-based intergrid transfer operator and abstract theories developed by Bramble et al. for non-nested multigrid algorithms.

The covolume-based intergrid transfer operators $I_k : V_{k-1} \rightarrow V_k$ for $k = 1, \dots, J$ are defined by

$$I_k v(P) = \sum_{i=1}^{N_{k-1}} v(P_i) |K_{P_i}^* \cap K_P^*| / |K_P^*|, \quad (3.3.1)$$

where P is a node point of \mathcal{T}_k and $|A|$ is the area of A .

REMARK 3.1. We consider Figure 2 as an example. Then

$$(I_k v)(P_5) = \frac{v(P_I) + v(P_{II})}{2}, \text{ and } (I_k v)(P_1) = v(P_I).$$

Compared to other intergrid transfer operators in [2](I_k^I) and [11](I_k^{II}),

$$\begin{aligned} (I_k^I v)(P_1) &= v(P_I) + \frac{1}{4}\{v(P_{II}) + v(P_{III}) - v(P_{IV}) - v(P_V)\} \\ (I_k^{II} v)(P_1) &= \frac{1}{2}v(P_I) + \frac{1}{4}\{v(P_{II}) + v(P_{III})\}, \end{aligned}$$

this operator needs less computation to compute values of nodes that are located in edges of the coarse grid.

REMARK 3.2. The intergrid transfer operator proposed in [2] cannot be employed in some nonlinear problems that have a restricted range of solution values and rapidly changing fields, such as the Marshak wave problem in radiation transport. If values of the solution are everywhere positive and $v(P_I)$, $v(P_{II})$ and $v(P_{III})$ are small and $v(P_{IV})$ and $v(P_V)$ are big, then $(I_k^I v)(P_1)$ is negative.

Let $A_k : V_k \rightarrow V_k$ be the discretization operator on level k given by

$$(A_k v, w)_k = a_k(v, w), \quad \forall v, w \in V_k.$$

The operator A_k is clearly symmetric (in both the $a_k(\cdot, \cdot)$ and (\cdot, \cdot) inner products) and positive definite. Also, we define the operators $P_{k-1}^0 : V_k \rightarrow V_{k-1}$ and $P_{k-1} : V_k \rightarrow V_{k-1}$ by

$$(I_k v, w) = (v, P_{k-1}^0 w), \quad \forall v \in V_{k-1}, \forall w \in V_k,$$

and

$$a_{k-1}(P_{k-1} w, v) = a_k(w, I_k v), \quad \forall v \in V_{k-1}, \forall w \in V_k.$$

It is easy to see that $I_k P_{k-1}$ is a symmetric operator with respect to the a_k form. Note that neither P_{k-1}^0 nor P_{k-1} is a projection in the nonconforming case.

REMARK 3.3. Because, for a coarse triangulation node P , $K_P^* \cap K_P^* = \emptyset$ except for six covolumes K_P maximally in a fine triangulation, the number of fine triangulation nodal values which need to calculate P_{k-1}^0 is less than six and this is less than the number of required fine triangulation nodal values in the intergrid transfer operator previously proposed in [2], [12]. As an example, we consider Figure 2. The transfer operator which was proposed in [2] requires the values of P_1, \dots, P_{14} ; and the transfer operator which was proposed in [11] requires the values of P_1, \dots, P_{10} to compute the value of P . But the transfer operator (3.3.1) needs only P_1, \dots, P_6 . Because, in the computation of I_k and P_{k-1}^0 , we need nodal values to calculate multiplication by the matrix A_k , this property is good for parallelization when the domain is partitioned by cutting edges between vertices and to preserve covolumes, so each vertex is uniquely owned.

Finally, let $R_k : V_k \rightarrow V_k$ for $k = 1, \dots, J$ be the linear smoothing operators, let R_k^T denote the adjoint of R_k with respect to the (\cdot, \cdot) inner product, and define

$$R_k^{(l)} = \begin{cases} R_k, & l \text{ odd}, \\ R_k^T, & l \text{ even}. \end{cases}$$

Following [3], the multigrid operator $B_k : V_k \rightarrow V_k$ is defined recursively as follows.

Multigrid Algorithm 3.1. Let $1 \leq k \leq J$ and p be a positive integer. Set $B_0 = A_0^{-1}$. Assume that B_{k-1} has been defined and define $B_k g$ for $g \in V_k$ by

- (1) Set $x^0 = 0$ and $q^0 = 0$.
- (2) Define x^l for $l = 1, \dots, m(k)$ by

$$x^l = x^{l-1} + R_k^{(l+m(k))}(g - A_k x^{l-1}).$$

- (3) Define $y^{m(k)} = x^{m(k)} + I_k q^p$, where q^i for $i = 1, \dots, p$ is defined by

$$q^i = q^{i-1} + B_{k-1}[P_{k-1}^0(g - A_k x^{m(k)}) - A_{k-1} q^{i-1}].$$

- (4) Define y^l for $l = m(k) + 1, \dots, 2m(k)$ by

$$y^l = y^{l-1} + R_k^{(l+m(k))}(g - A_k y^{l-1}).$$

- (5) Set $B_k g = y^{2m(k)}$.

In Multigrid algorithm 2.1, $m(k)$ gives the number of pre- and post-smoothing iterations and can vary as a function of k . If $p = 1$, we have a V -cycle multigrid algorithm. If $p = 2$, we have a W -cycle multigrid algorithm. Other versions of multigrid algorithms without pre- or post-smoothing iterations can be analyzed similarly. A variable V -cycle multigrid algorithm is that for which the number of smoothing $m(k)$ increases exponentially as k decreases (i.e., $p = 1$ and $m(k) = 2^{J-k}$).

Based on the methodology developed in [3], two other very important ingredients in convergence analysis of non-nested multigrid algorithms are the following assumptions.

A.1: (Regularity and approximation assumption) For some $\alpha \in (0, 1]$ there exists C_α , independent of k , such that

$$|a_k(v - I_k P_{k-1} v, v)| \leq C_\alpha \left(\frac{\|A_k v\|^2}{\lambda_k} \right)^\alpha a_k(v, v)^{1-\alpha}, \quad (3.3.2)$$

where λ_k is the maximum eigenvalue of A_k .

A.2: There exists $C_R \geq 1$, independent of k , such that

$$\frac{\|u\|^2}{\lambda_k} \leq C_R(\bar{R}_k u, u), \forall u \in V_k,$$

where $\bar{R}_k = (I - K_k^* K_k) A_k^{-1}$ and $K_k = I - R_k A_k$ and K_k^* is an adjoint of K_k with respect to $a_k(\cdot, \cdot)$.

THEOREM 3.4. *Let B_k be defined by Algorithm 2.1. Suppose that A.1 and A.2 hold. Let $p = 2$ and $m(k) = m$ for all k . Then, for m sufficiently large, there is a constant M independent of m such that*

$$|a_k((I - B_k A_k)u, u)| \leq \delta A_k(u, u), \quad \forall u \in V_k,$$

with

$$\delta \leq \frac{M}{M + m^\alpha}.$$

REMARK 3.5. *Theorem 3.1 shows that the convergence factor of the W -cycle multigrid algorithm does not depend the number of levels if the multigrid method is convergent.*

The following result concerns the variable V -cycle multigrid algorithm.

THEOREM 3.6. *Let B_k be defined by Algorithm 2.1. Suppose that A.1 and A.2 hold. The number of smoothings, $m(k)$, increases as k decreases in such a way that*

$$\beta_0 m(k) \leq m(k-1) \leq \beta_1 m(k)$$

with $1 < \beta_0 \leq \beta_1$. Let $p = 1$. Then

$$\eta_0 a_k(u, u) \leq a_k(B_k A_k u, u) \leq \eta_1 a_k(u, u), \quad \forall u \in V_k$$

holds with $\eta_0 \geq \frac{m(k)^\alpha}{M+m(k)^\alpha}$ and $\eta_1 \leq \frac{M+m(k)^\alpha}{m(k)^\alpha}$ for some $M > 0$.

REMARK 3.7. *The convergence of V-cycle multigrid algorithm is difficult to show. However, in many numerical experiments, the V-cycle multigrid algorithm also converges if the number of smoothings m is sufficiently large.*

4. Numerical results. In this section, we consider two second-order elliptic problems and compare the convergence behavior of multigrid algorithms with a covolume-based intergrid transfer operator and other intergrid transfer operators on P_1 -nonconforming multigrid algorithms.

Example 1. We consider the Laplace equation on the unit square

$$\begin{aligned} -\Delta u &= f, & \text{in } \Omega, \\ \beta u + \frac{\partial u}{\partial n} &= g, & \text{on } \partial\Omega, \end{aligned} \tag{4.4.1}$$

where

$$\beta = \begin{cases} 0 & \text{at } y = 0, 1 \\ 1 & \text{at } x = 0, 1 \end{cases}$$

and the coarsest primal triangulation of Ω is shown Figure 3(a).

In Figure 3, we show some primal triangulations which generated by the nested-mesh subdivision method. We compare convergence rates of W -cycle multigrid methods with with intergrid transfer operator I_k , intergrid transfer operator I_k^I , which was defined in [2], and intergrid transfer operator I_k^{II} , which was defined in [11] in Figure 4(a) and 4(b). We perform 3 Gauss-Seidel sweeps in Figure 4(a) and 4 damped Jacobi sweeps with damping coefficient $\omega = 0.6$ in Figure 4(b). These figures show that the error reduction of I_k^{II} is very poor for the Robin or the Neumann boundary value problem.

We report the average error reduction of the W -cycle multigrid method with the covolume based intergrid transfer operator with respect to number of grid levels in Table 1(a) for the Gauss-Seidel smoother and Table 1(b) for the damped Jacobi smoother. For reference, we report that the average error reduction of the V -cycle multigrid method Table 1(c) and (d).

REMARK 4.1. *Table 1 shows that the average error reduction of the W -cycle multigrid method does not depend the number of grid levels but that of the V -cycle multigrid method does depend on the number of levels. Also, Table 1 shows that the V -cycle multigrid method converges for a sufficient number of smoothing steps.*

In Figure 5, we compare convergence rates of the Preconditioned Conjugate Gradient method with multigrid as a preconditioner. Also, we report in Table 2 the average error reduction of PCG with P_1 nonconforming multigrid algorithm as a preconditioner.

REMARK 4.2. *Table 2 shows that the average error reduction of PCG with variable V -cycle multigrid as a preconditioner does not depend the number of grid levels, but a V -cycle multigrid algorithm does depend on the number of levels.*

Example 2. We consider the second-order partial differential equation with discontinuous coefficients

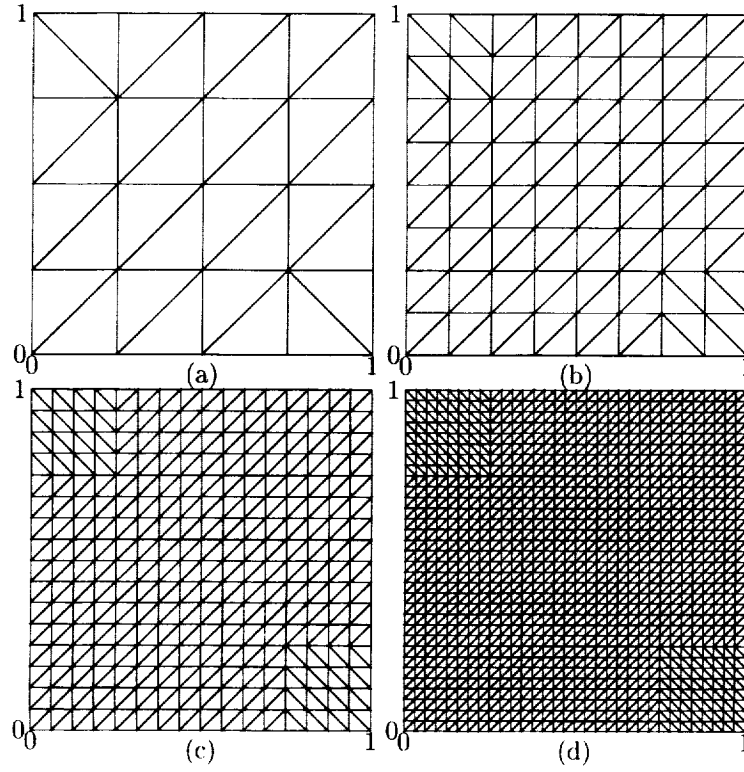


FIG. 3. Discretization for example 1

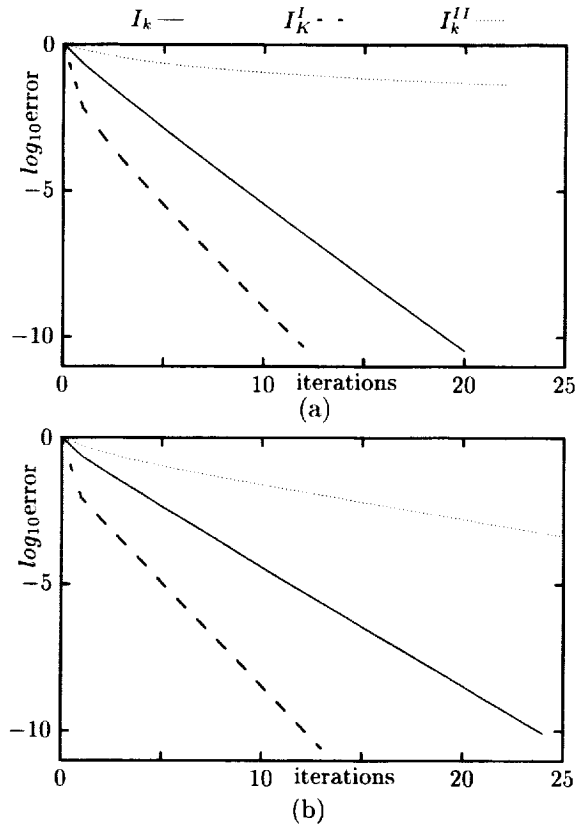


FIG. 4. Comparison of error reduction of the W-cycle multigrid method. (a) Using 3 Gauss-Seidel smoothing steps per level. (b) Using 4 Damped Jacobi smoothing steps with $\omega = 0.6$ per level

TABLE 1. Average error reductions of multigrid method. (a) W-cycle multigrid with Gauss-Seidel smoother. (b) W-cycle multigrid with Jacobi smoother. (c) V-cycle multigrid with Gauss-Seidel smoother. (d) V-cycle multigrid with Jacobi smoother. (* : not converge)

$J \backslash m$	1	2	3	4	5
3	0.667	0.391	0.294	0.185	0.135
4	0.657	0.386	0.300	0.179	0.137
5	0.677	0.377	0.300	0.173	0.137
6	0.677	0.367	0.300	0.165	0.136
7	0.677	0.360	0.300	0.160	0.136

(a)

$J \backslash m$	1	3	5	7	9
3	0.778	0.492	0.325	0.221	0.153
4	0.781	0.489	0.319	0.213	0.146
5	0.782	0.484	0.311	0.207	0.140
6	0.782	0.482	0.306	0.201	0.135
7	0.782	0.480	0.303	0.197	0.131

(b)

$J \backslash m$	3	4	5	6	7
3	0.420	0.251	0.168	0.152	0.093
4	0.496	0.264	0.184	0.161	0.105
5	0.572	0.272	0.196	0.166	0.112
6	0.646	0.276	0.204	0.169	0.117
7	0.720	0.281	0.214	0.174	0.121

(c)

$J \backslash m$	4	5	6	7	8
3	0.535	0.416	0.346	0.291	0.246
4	0.681	0.503	0.378	0.308	0.261
5	0.825	0.592	0.432	0.326	0.270
6	0.973	0.677	0.484	0.353	0.278
7	*	0.761	0.535	0.384	0.288

(d)

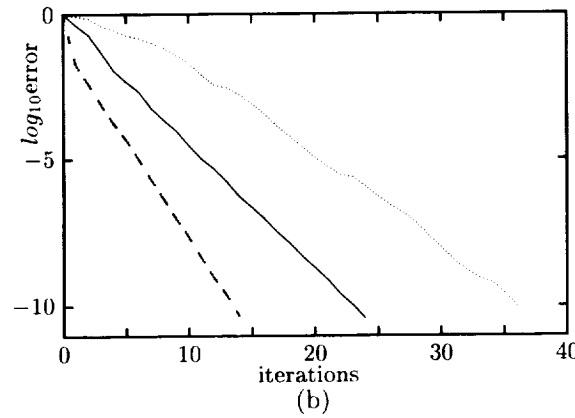
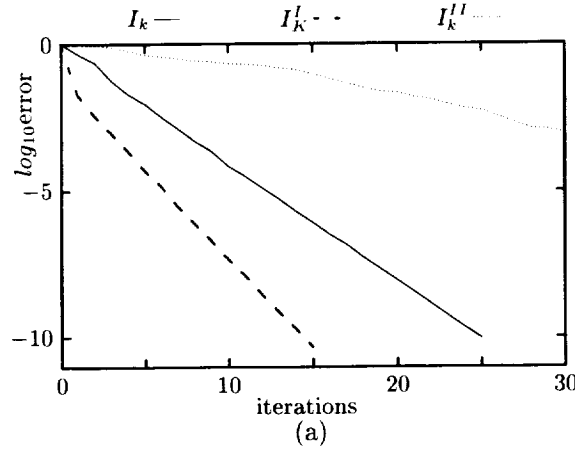


FIG. 5. Comparison of error reduction of Preconditioned CG. (a) Using 1 Gauss-Seidel smoothing step per level. (b) Using 2 Damped Jacobi smoothing steps with $\omega = 0.6$ per level

TABLE 2. Average error reductions of Preconditioned CG. (a) Variable V-cycle multigrid with Gauss-Seidel smoother. (b) Variable V-cycle multigrid with Jacobi smoother. (c) V-cycle multigrid with Gauss-Seidel smoother. (d) V-cycle multigrid with Jacobi smoother

$J \setminus m(J)$	1	2	3	4
3	0.380	0.175	0.147	0.077
4	0.387	0.179	0.154	0.078
5	0.392	0.181	0.156	0.078
6	0.395	0.181	0.156	0.078
7	0.397	0.182	0.157	0.077

(a)

$J \setminus m(J)$	1	2	3	4
3	0.510	0.358	0.262	0.202
4	0.526	0.362	0.267	0.206
5	0.535	0.366	0.267	0.207
6	0.540	0.367	0.269	0.208
7	0.542	0.368	0.270	0.207

(b)

$J \setminus m$	1	2	3	4
3	0.490	0.226	0.205	0.104
4	0.546	0.242	0.229	0.110
5	0.593	0.256	0.249	0.116
6	0.634	0.268	0.265	0.121
7	0.668	0.278	0.280	0.124

(c)

$J \setminus m$	1	2	3	4
3	0.563	0.433	0.347	0.281
4	0.615	0.475	0.387	0.312
5	0.660	0.521	0.420	0.340
6	0.696	0.559	0.451	0.363
7	0.732	0.590	0.476	0.385

(d)

on the unit square

$$\begin{aligned} -\nabla \cdot \mathbb{A} \nabla u &= f, & \text{in } \Omega, \\ \beta u + \mathbb{A} \frac{\partial u}{\partial n} &= g, & \text{on } \partial \Omega, \end{aligned} \quad (4.4.2)$$

where

$$\mathbb{A}(x, y) = \begin{cases} 10, & \text{if } 1/3 \leq x \leq 2/3 \text{ and } 1/3 \leq y \leq 2/3, \\ 1, & \text{otherwise,} \end{cases}$$

β is the same value as in Example 1 and the coarsest primal triangulation of Ω is shown Figure 6(a).

In Figure 6, we show some primal triangulations which generated by the nested-mesh subdivision method.

In Figure 7 and 8 and Table 3 and 4, we report the same numerical experiments applied to (4.4.2). In these numerical experiments, the error reduction factor slightly increases in the W-cycle multigrid method and PCG with variable V-cycle multigrid preconditioner, but is not rapidly increasing compared with V-cycle multigrid and PCG with a V-cycle multigrid preconditioner. This result is related to the regularity of the partial differential equation.

Example 3. As a nonlinear example, we consider a non-equilibrium radiation diffusion equation system, which can be written as

$$\begin{aligned} \frac{\partial E}{\partial t} - \nabla \cdot (D_r \nabla E) &= \sigma_a (T^4 - E), & \text{in } \Omega, \\ \frac{\partial T}{\partial t} - \nabla \cdot (D_t \nabla T) &= -\sigma_a (T^4 - E), & \text{in } \Omega, \end{aligned} \quad (4.4.3)$$

with

$$\sigma_a = \frac{z^3}{T^3}, \quad D_r(T, E) = \frac{1}{3\sigma_a + \frac{1}{E} |\nabla E|}, \quad D_t(T) = \kappa T^{\frac{5}{2}}.$$

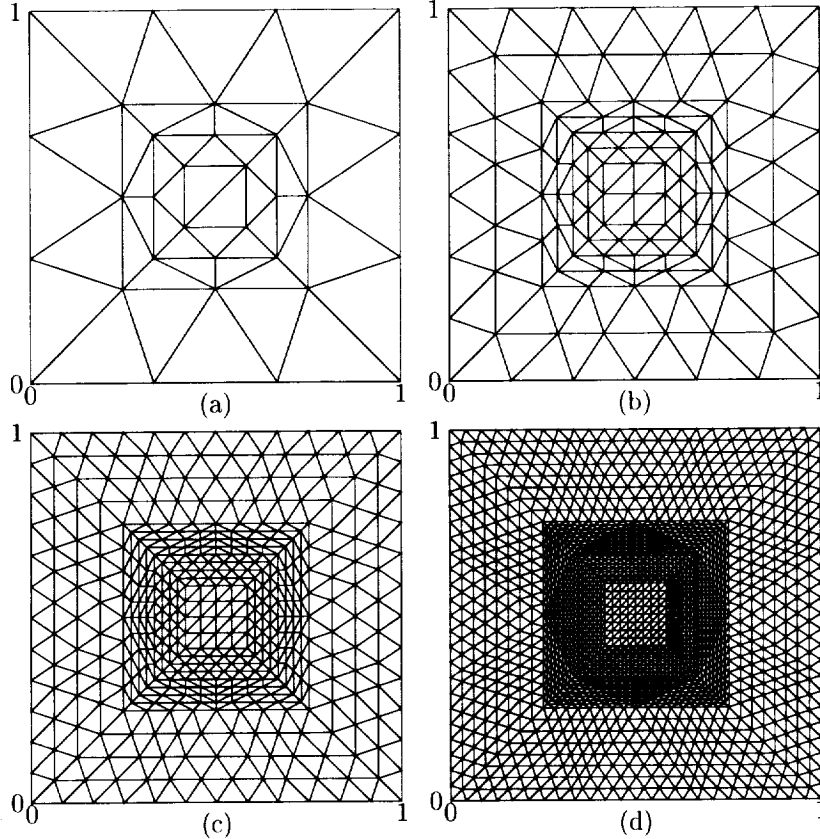


FIG. 6. *Discretization for example 2*

Here, E represents the photon energy, T is the material temperature, and κ is the material conductivity. In the non-equilibrium case, the nonlinear source terms on the right-hand-side are nonzero and govern the transfer of energy between the radiation field and material temperature. Additional nonlinearities are generated by the particular form of the diffusion coefficients, which are functions of the E and T variables. In particular, the energy diffusion coefficient, $D_r(T, E)$ contains the term $|\nabla E|$ which refers to the gradient of E . This limiter term is an artificial means of ensuring physically meaningful energy propagation speeds (i.e. no signal speeds faster than the speed of light) ([16, 13, 15]). The atomic number z is a material coefficient, and while it may be highly variable, it is a function of position only (i.e. $z = f(x, y)$ in two dimensions).

Equations (4.4.3) represent a system of coupled nonlinear partial differential equations which must be discretized in space and time. The time derivatives are discretized as first-order backwards differences, with lumping of the mass matrix, leading to an implicit scheme which requires the solution of a nonlinear problem at each time step. This approach is first-order accurate in time, and is chosen merely for convenience, since the principal objective is the study of the solution of the nonlinear system. Spatial discretization on two-dimensional triangular meshes is achieved by a P_1 -nonconforming finite element procedure, assuming linear variations of E and T over a triangular element.

The test case chosen for this work is taken from [16, 15], we consider a unit square domain of two dissimilar materials, where the outer region contains an atomic number of $z = 1$ and the inner region ($1/3 < x < 2/3, 1/3 < y < 2/3$) contains an atomic number of $z = 10$. The top and bottom walls are insulated, and inlet outlet boundaries are specified using mixed Robin boundary conditions, as shown in the Figure 9. We use the same triangulation to the previous example 2.

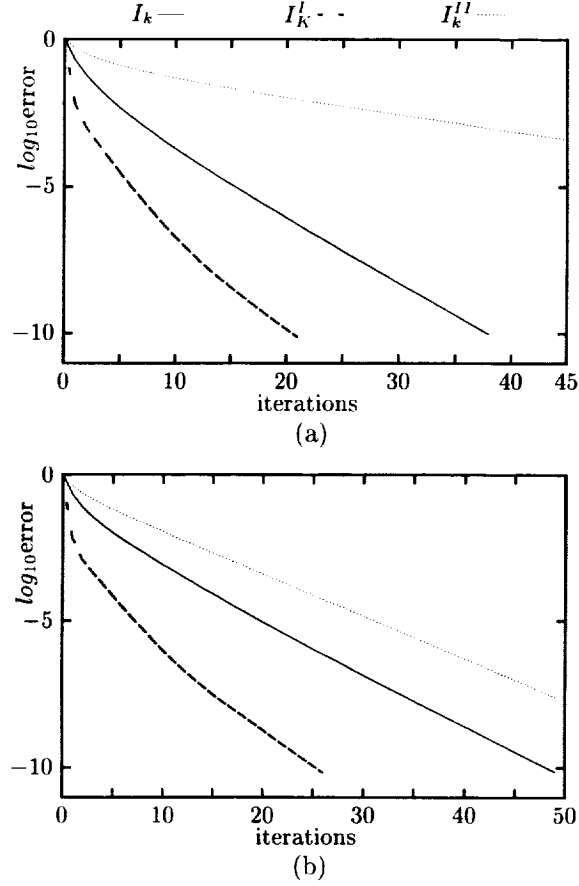


FIG. 7. Comparison of error reduction of the W-cycle multigrid method. (a) Using 3 Gauss-Seidel smoothing steps per level. (b) Using 4 Damped Jacobi smoothing steps with $\omega = 0.6$ per level

TABLE 3. Average error reductions of multigrid method. (a) W-cycle multigrid with Gauss-Seidel smoother. (b) W-cycle multigrid with Jacobi smoother. (c) V-cycle multigrid with Gauss-Seidel smoother. (d) V-cycle multigrid with Jacobi smoother. (*: not converge)

$J \backslash m$	1	2	3	4	5
3	0.783	0.527	0.498	0.311	0.330
4	0.801	0.549	0.525	0.343	0.357
5	0.812	0.557	0.539	0.350	0.366
6	0.818	0.560	0.545	0.355	0.372

(a)

$J \backslash m$	1	3	5	7	9
3	0.857	0.646	0.511	0.412	0.340
4	0.872	0.675	0.542	0.445	0.371
5	0.880	0.689	0.553	0.454	0.377
6	0.885	0.696	0.557	0.452	0.375

(b)

$J \backslash m$	3	5	7	9	11
3	0.564	0.358	0.245	0.169	0.120
4	0.722	0.403	0.285	0.203	0.145
5	0.886	0.473	0.313	0.226	0.164
6	*	0.680	0.409	0.264	0.182

(c)

$J \backslash m$	4	6	8	10	12
3	0.759	0.492	0.394	0.326	0.270
4	0.967	0.624	0.447	0.376	0.316
5	*	0.751	0.501	0.408	0.346
6	*	0.874	0.567	0.432	0.366

(d)

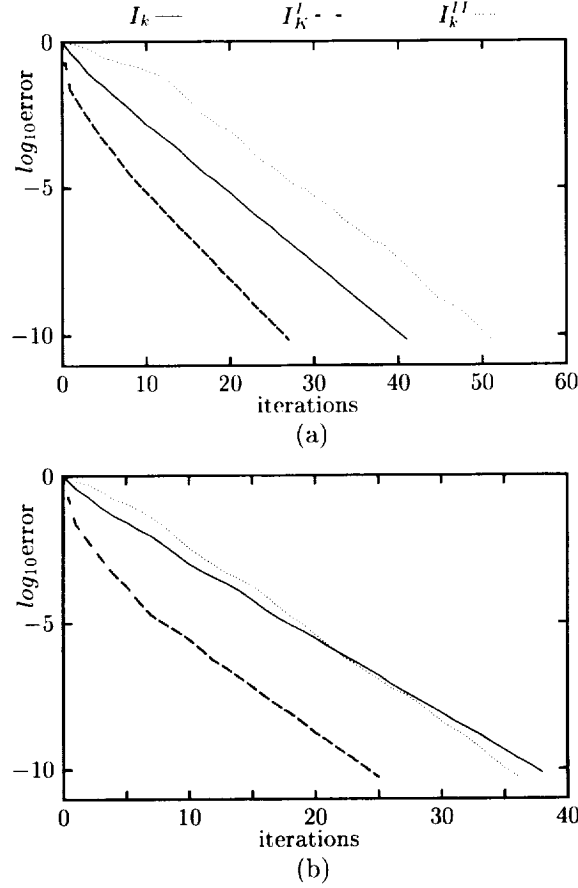


FIG. 8. Comparison of error reduction of Preconditioned CG. (a) Using 1 Gauss-Seidel smoothing step per level. (b) Using 2 Damped Jacobi smoothing steps with $\omega = 0.6$ per level

TABLE 4. Average error reductions of Preconditioned CG. (a) Variable V-cycle multigrid with Gauss-Seidel smoother. (b) Variable V-cycle multigrid with Jacobi smoother. (c) V-cycle multigrid with Gauss-Seidel smoother. (d) V-cycle multigrid with Jacobi smoother

$J \setminus m(J)$	1	2	3	4
3	0.516	0.299	0.268	0.161
4	0.541	0.311	0.282	0.173
5	0.557	0.314	0.293	0.178
6	0.566	0.315	0.301	0.178

(a)

$J \setminus m(J)$	1	2	3	4
3	0.614	0.465	0.372	0.309
4	0.647	0.499	0.405	0.343
5	0.674	0.527	0.429	0.357
6	0.690	0.541	0.442	0.371

(b)

$J \setminus m$	1	2	3	4
3	0.579	0.327	0.305	0.191
4	0.632	0.363	0.351	0.219
5	0.676	0.388	0.391	0.231
6	0.716	0.412	0.439	0.245

(c)

$J \setminus m$	1	2	3	4
3	0.641	0.500	0.413	0.351
4	0.699	0.558	0.469	0.408
5	0.742	0.606	0.515	0.449
6	0.777	0.643	0.554	0.486

(d)

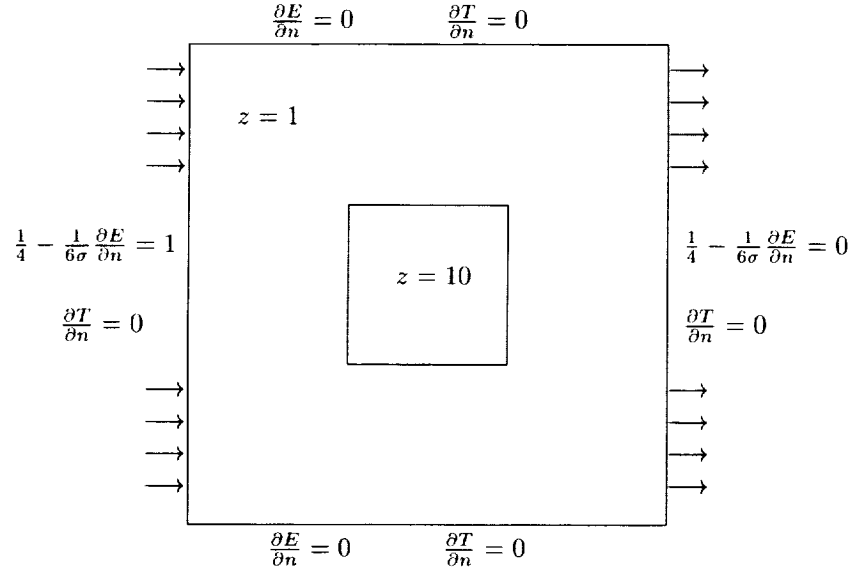


FIG. 9. *Test problem for radiation transport problem*

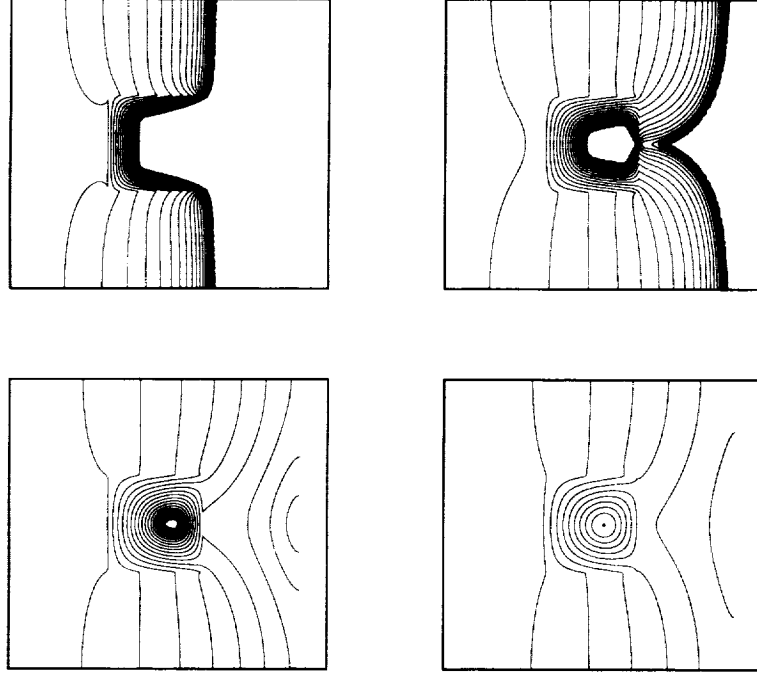


FIG. 10. *Some numerical results of radiation transport problem*

This problem is highly nonlinear and has been identified as one of the most time-consuming components in large multiphysics simulation codes. To solve this nonlinear problem, we use Newton linearization method. However the resulting linear problems are nonsymmetric, so we use Preconditioned GMRES(PGMRES) with a nonconforming multigrid preconditioner (V -cycle or the variable V -cycle multigrid algorithm defined in section 3) to solve the linear problem. In Figure 10, we illustrate a typical simulation result for this system.

We plot the contour of temperature T at time $t = 2.0, 3.0, 4.0, 5.0$. These show that the solutions are rapidly changing near the position where the two different materials meet.

To get the coarse grid operators, we need to get some approximations in the coarse finite element space of solutions in the finest finite element space. When we use $(I_k^I)^T$ as the fine-to-coarse intergrid transfer operator, we cannot solve some coarse level problems because coarse level bilinear operator fails to be defined (some values of temperature T are negative, as remark 3.2), or the coarse level problem is very hard to solve by using iterative methods. But, if we use $(I_k)^T$ as fine-to-coarse intergrid transfer operator, the preconditioners work well.

In Figure 11, we compare the error reduction of PGMRES with V -cycle and variable V -cycle with smoothing number 1 and 2 and Gauss-Seidel smoothing at time $t = 2.0$ with time step size $dt = 0.001, 0.002, 0.005, 0.01$. We measure linear residual error by preconditioned error and stop the linear PGMRES iteration if the relative linear residual error is less than 10^{-6} . For each time step, we stop the nonlinear iteration if the nonlinear residual error is less than 5×10^{-5} .

The numerical results at time $t = 2.0$ show that there is no significant difference between V -cycle and variable V -cycle preconditioner, but significant improvement in error reduction in solving the linear problem when one increases the smoothing number.

We have a studied covolume-based intergrid transfer operators in a P_1 nonconforming multigrid. We found that multigrid methods with covolume-based intergrid transfer operators converge more slowly than with a standard previous intergrid transfer operator. This result was expected because this operator is simple and does not preserve as many high-order functions as the standard operator. However, we promote this operator for preservation of positivity in solving nonlinear problems and for parallelization.

Acknowledgments. The author would like to thank D. E. Keyes of Old Dominion University for his valuable advice in the preparation of this paper.

REFERENCES

- [1] R. Bank and T. Dupont, *An optimal order process for solving finite element equations*, Math. Comp., **36**(1981), pp. 35–51.
- [2] D. Braess and R. Verfürth, *Multigrid methods for nonconforming finite elements methods*, SIAM J. Numer. Anal., **27**(1990), pp. 979–986.
- [3] J. Bramble, *Multigrid Methods*, Pitman, London, 1993.
- [4] J. Bramble, J. Pasciak, and J. Xu, *The analysis of multigrid algorithms with non-nested spaces or non-inherited quadratic forms*, Math. Comp., **56**(1991), pp. 1–34.
- [5] A. Brandt, *Multigrid techniques with applications to fluid dynamics: 1984 guide*, in VKI Lecture Series, Mar. 1984, 176 pp.
- [6] S. Brenner, *An optimal-order multigrid method for P_1 nonconforming finite elements*, Math. Comp., **52**(1989), pp. 1–15.
- [7] S. Brenner, *An optimal order nonconforming multigrid method for the biharmonic equation*, SIAM J. Numer. Anal., **26**(1989), pp. 1124–1138.
- [8] S. H. Chou, *Analysis and convergence of a covolume method for the generalized Stokes Problem*, Math. Comp., **66**(1989), pp. 85–104.
- [9] M. Crouzeix and P. A. Raviart, *Conforming and nonconforming finite element method for solving the stationary Stokes equations. I*, RAIRO R-3 (1973), pp. 33–75.

- [10] W. Hackbush, *Multigrid Methods and Applications*, Springer-Verlag, Berlin, Germany, 1985.
- [11] K. S. Kang and D. Y. Kwak, *Error estimate in L^2 of a covolume method for the generalized Stokes problem*, submitted to Numerical Methods for Partial Differential Equations.
- [12] K. S. Kang and S. Y. Lee, *New intergrid transfer operator in multigrid method for P_1 -nonconforming finite element method*, Applied Mathematics and Computation, **100**(1999), pp. 139–149.
- [13] D. A. Knoll, W. J. Rider, and G. L. Olson, *An efficient nonlinear solution method for nonequilibrium radiation diffusion*, J. Quant. Spec. and Rad. Trans., **63**(1999), pp. 15–29.
- [14] D. J. Mavriplis, *Multigrid techniques for unstructured meshes*, in VKI Lecture Series VKI-LS 1995-02, Mar. 1995.
- [15] D. J. Mavriplis, *An Assessment of Linear Versus Non-linear Multigrid Methods for Unstructured Mesh Solvers*, ICASE Report No. 2001-12, 2001.
- [16] V. A. Mousseau, D. A. Knoll, and W. J. Rider, *Physics-based preconditioning and the Newton-Krylov method for non-equilibrium radiation diffusion*, Journal of Computational Physics, **160**(2000), pp. 743–765.
- [17] P. Wesseling, *An Introduction to Multigrid Methods*, Wiley, Chichester, U.K., 1992.

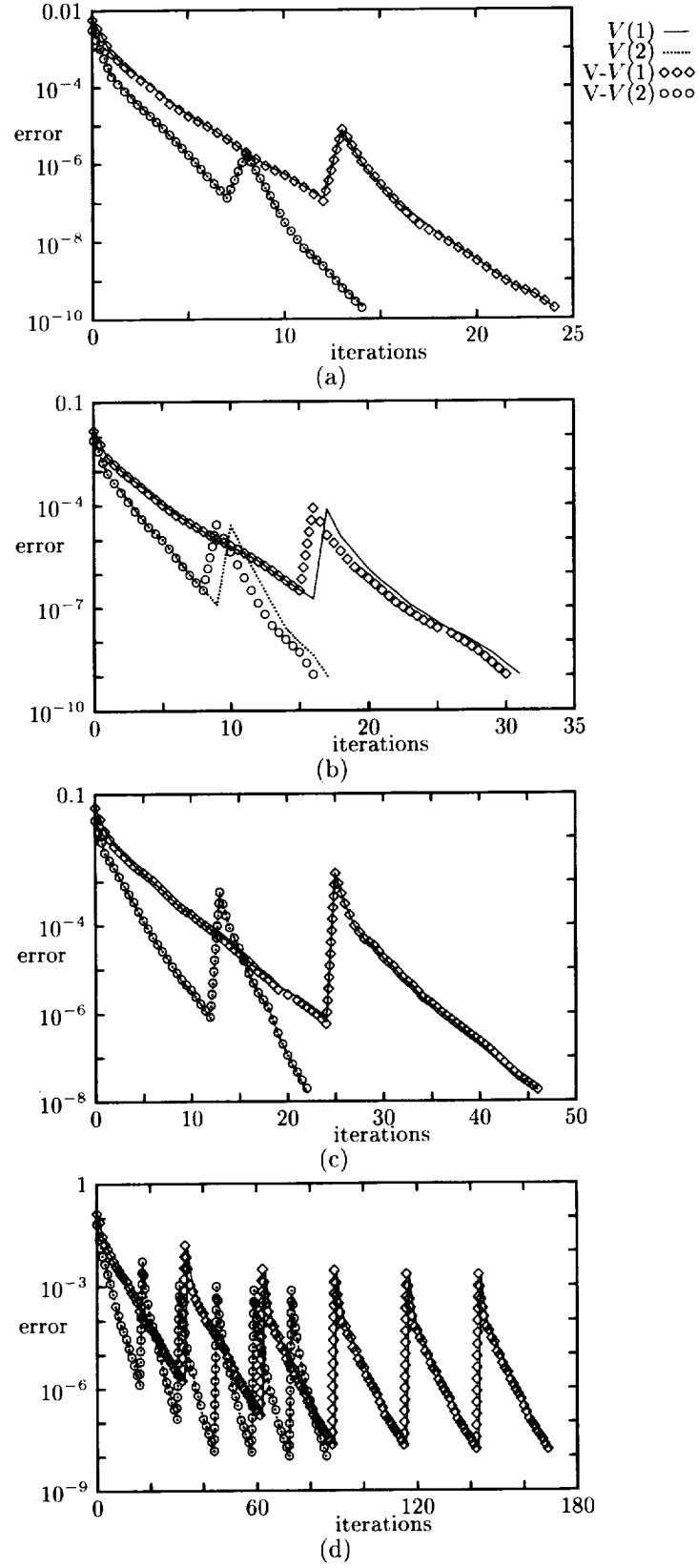


FIG. 11. Error reduction of PGMRES at $t = 2.0$. (a) $dt = 0.001$. (b) $dt = 0.002$. (c) $dt = 0.005$. (d) $dt = 0.01$

REPORT DOCUMENTATION PAGE			Form Approved OMB No. 0704-0188	
Public reporting burden for this collection of information is estimated to average 1 hour per response, including the time for reviewing instructions, searching existing data sources, gathering and maintaining the data needed, and completing and reviewing the collection of information. Send comments regarding this burden estimate or any other aspect of this collection of information, including suggestions for reducing this burden, to Washington Headquarters Services, Directorate for Information Operations and Reports, 1215 Jefferson Davis Highway, Suite 1204, Arlington, VA 22202-4302, and to the Office of Management and Budget, Paperwork Reduction Project (0704-0188), Washington, DC 20503.				
1. AGENCY USE ONLY(Leave blank)		2. REPORT DATE May 2002		3. REPORT TYPE AND DATES COVERED Contractor Report
4. TITLE AND SUBTITLE Covolume-based intergrid transfer operator in P_1 nonconforming multigrid method			5. FUNDING NUMBERS C NAS1-97046 WU 505-90-52-01	
6. AUTHOR(S) Kab Seok Kang				
7. PERFORMING ORGANIZATION NAME(S) AND ADDRESS(ES) ICASE Mail Stop 132C NASA Langley Research Center Hampton, VA 23681-2199			8. PERFORMING ORGANIZATION REPORT NUMBER ICASE Report No. 2002-15	
9. SPONSORING/MONITORING AGENCY NAME(S) AND ADDRESS(ES) National Aeronautics and Space Administration Langley Research Center Hampton, VA 23681-2199			10. SPONSORING/MONITORING AGENCY REPORT NUMBER NASA/CR-2002-211655 ICASE Report No. 2002-15	
11. SUPPLEMENTARY NOTES Langley Technical Monitor: Dennis M. Bushnell Final Report To be submitted to Applied Numerical Mathematics.				
12a. DISTRIBUTION/AVAILABILITY STATEMENT Unclassified-Unlimited Subject Category 64 Distribution: Nonstandard Availability: NASA-CASI (301) 621-0390			12b. DISTRIBUTION CODE	
13. ABSTRACT (Maximum 200 words) In this paper, we introduce an intergrid transfer operator which is based on the covolume of nodes in a P_1 nonconforming multigrid method and study the convergence behavior of the multigrid method with this intergrid transfer operator. This intergrid transfer operator needs fewer computations and neighborhood node values than previous operators, which is a good property for parallelization. The P_1 nonconforming multigrid method with this intergrid transfer operator is suitable for solving problems with Robin boundary conditions and nonlinear problems with bound constraints on solutions.				
14. SUBJECT TERMS multigrid method, covolume method, nonconforming finite elements, elliptic equations			15. NUMBER OF PAGES 22	
			16. PRICE CODE A03	
17. SECURITY CLASSIFICATION OF REPORT Unclassified		18. SECURITY CLASSIFICATION OF THIS PAGE Unclassified		19. SECURITY CLASSIFICATION OF ABSTRACT
				20. LIMITATION OF ABSTRACT